

Effective Parameters Controlling Sterol Transfer: A Time-Resolved Small-Angle Neutron Scattering Study

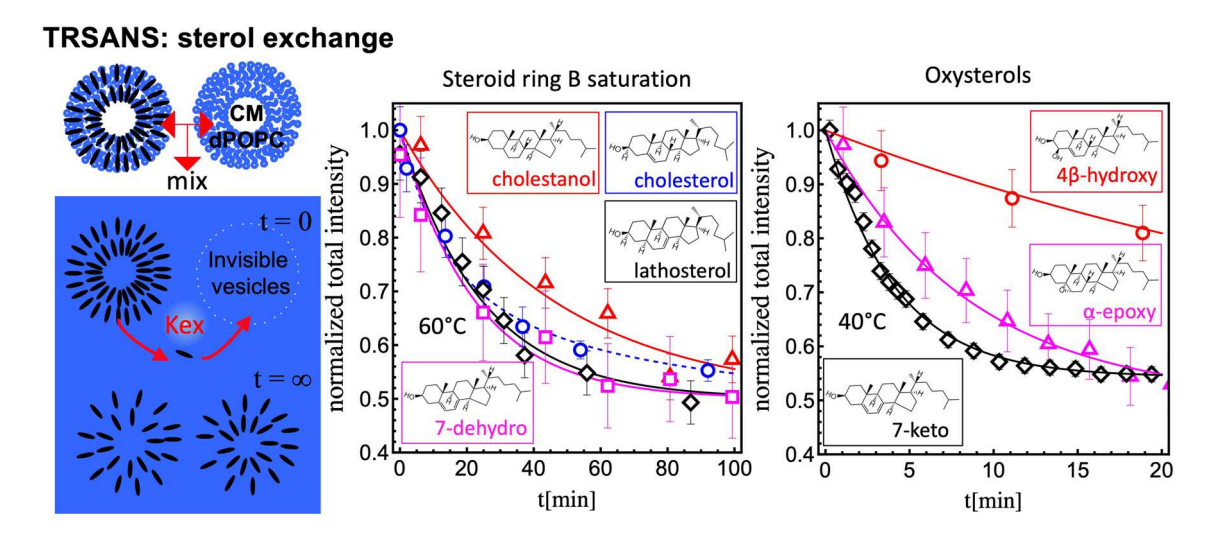
Ursula Perez-Salas¹ · Lionel Porcar² · Sumit Garg¹ · Manuela A. A. Ayee³ · Irena Levitan⁴

Received: 25 December 2021 / Accepted: 19 March 2022 / Published online: 25 April 2022 © The Author(s), under exclusive licence to Springer Science+Business Media, LLC, part of Springer Nature 2022

Abstract

Though cholesterol is the most prevalent and essential sterol in mammalian cellular membranes, its precursors, post-synthesis cholesterol products, as well as its oxidized derivatives play many other important physiological roles. Using a non-invasive in situ technique, time-resolved small angle neutron scattering, we report on the rate of membrane desorption and corresponding activation energy for this process for a series of sterol precursors and post-synthesis cholesterol products that vary from cholesterol by the number and position of double bonds in B ring of cholesterol's steroid core. In addition, we report on sterols that have oxidation modifications in ring B of the steroid core. We find that sterols that differ in position or the number of double bonds in ring B have similar time and energy characteristics, while oxysterols have faster transfer rates and lower activation energies than cholesterol in a manner generally consistent with known sterol characteristics, like Log P, the n-octanol/water partitioning coefficient. We find, however, that membrane/water partitioning which is dependent on lipid-sterol interactions is a better predictor, shown by the correlation of the sterols' tilt modulus with both the desorption rates and activation energy.

Graphic Abstract



Keywords Cholesterol · Oxysterols · Lipid transfer · Lipid exchange · Lipid flip-flop

Extended author information available on the last page of the article

Introduction

Cholesterol is the most prevalent and essential sterol in mammalian cellular membranes (Maxfield and Meer 2010). In the plasma membrane (PM), cholesterol is the most



 [□] Ursula Perez-Salas ursulaps@uic.edu

abundant single component (~40 mol%), with more than double the amount of phospholipids (Lorent et al. 2020). Diverse cellular functions require cholesterol, including participating in the formation of lipid rafts (Brown and London 1998a) which are implicated in multiple cellular responses ranging from physiological to pathological (Sviridov et al. 2020; Ripa et al. 2021), as well as binding to sterol-sensing domains to regulate protein function (Epand 2006), or in signal transduction across the PM (Sheng et al. 2012). Biochemically, cholesterol serves as a precursor for the synthesis of steroid hormones (Hu et al. 2010) and bile acid (Chiang 2004). Therefore, even a small change in the chemical structure of cholesterol can have a significant effect on membrane structure and function (Bloch 1983; Xu and London 2000; Delle Bovi et al. 2019), and dynamics (Dufourc 2008) and can lead to lethal diseases (Shrivastava et al. 2020). Yet, a more diverse view in which other sterols contribute to the complexity of biological function by their structural heterogeneity, and leading to differences in membrane behavior from those imparted by cholesterol is also of critical importance (Maxfield and Mondal 2006; Spann and Glass 2013; Ayee and Levitan 2021). In addition, other organisms, lacking cholesterol, modulate membrane function by a diverse family of sterols (Nes 2011).

Several studies have been pursued to understand the class of structural differences in sterols that lead to similarities and differences with cholesterol (Serfis et al. 2001; Shaghaghi et al. 2016). Most of the studies have focused on characterizing the in-plane packing of lipids with different sterols and in particular track the ability (or not) of sterols to condense lipids around them—by virtue of a flat tetracyclic carbon ring core—which results in enhanced membrane thickness as well as the formation of a liquid-ordered phase, both factors that enable the formation of lipid domains (Xu and London 2000; Bernsdorff and Winter 2003; Wang and Megha 2004; Bacia et al. 2005; Megha and Bakht 2006; Shentu et al. 2010).

In addition to lipid packing and in-plane lipid sorting effects, another important characteristic of lipids is their translocation characteristics. The cell is known to maintain a complex homeostatic transport network for sterols (Yamauchi and Rogers 2018; Ikonen and Zhou 2021; Menon 2018; Winkler et al. 2019); however, unassisted transport across an aqueous environment without the need of active transporters or membrane contact/proximity is certainly possible (Garg et al. 2011; McLean and Phillips 1981; Phillips et al. 1987). A recent simulation study by Atkovska et al., which looked at over thirty sterol species, showed that both the exit characteristics into the surrounding aqueous environment as well as the movement across a lipid bilayer of sterols can vary by many orders of magnitude depending on the sterol structure (Atkovska et al. 2018). In their simulation, for example, cholesterol exit times are slow, but their intra-leaflet mobility is fast. In contrast, hydrocortisone can move through the aqueous environment fast but will translocate slowly in the lipid bilayer. Indeed, the timescale of desorption rates for sterols like cholesterol is found to be slow experimentally (Garg et al. 2011). Hence mapping out the structure characteristics that lead to specific transport behavior will provide insight into the cell's strategies to move these lipids across cellular membranes.

Here, we present a study of the desorption/transfer characteristics of different sterols between POPC membranes using a non-invasive in situ technique: time-resolved small angle neutron scattering (TR-SANS). TR-SANS was initially applied to study the exchange rate of polymer chains between polymer micelles (Lund et al. 2006) and shortly after established for the exchange of lipids within vesicles (Nakano et al. 2007) and has since been used by several groups, as reviewed recently by Perez-Salas et al. (2021). The sterols in the current study were chosen not only for their structural similarities to cholesterol but also for their implications in several diseases, where differences in transfer characteristics between membranes may play an important role.

The first group of sterols we studied looked at the effect of changing the number of double bonds in ring B (see Fig. 1) where we have either two double bonds (7-dehydrocholesterol), one double bond but in a different location than cholesterol (lathosterol) or none (cholestanol). Cholestanol is derived from cholesterol and bile derivatives in the liver (Skrede et al. 1985), but the capacity of this pathway is low; when accumulated in large amounts in the brain and other tissues, it produces cerebrotendinous xanthomatosis. Lathosterol and 7-dehydrocholesterol are late precursors in cholesterol's biosynthetic pathways. 7-dehydrocholesterol is synthesized from lathosterol adding an additional double bond at C5–C6, while lathosterol has only a double bond at C7–C8 (Fig. 1). Accumulation of 7-dehydrocholesterol, due to a mutation in the enzyme that catalyzes its reduction to cholesterol, termed the Smith-Lemli-Opitz syndrome, has fatal congenital malformations (Porter 2002). Similarly, albeit they are similar in their chemical structures, the accumulation of lathosterol gives rise to lathosterolosis, which is another fatal malformation syndrome (Krakowiak et al. 2003).

Additionally, we report on the membrane transfer behavior of a second group of sterols: oxysterols, which are cholesterol-derived compounds with additional oxygen substitutions, commonly hydroxyl, carbonyl, or epoxy groups. Herein, we studied oxysterols with side-group modifications in either ring A, 48-hydroxycholesterol, or ring B, 5α , 6α -epoxycholesterol and 7-ketocholesterol (Fig. 1). Oxysterols are potent regulators of cellular lipid homeostasis (Olkkonen et al. 2012), and as such, they can contribute to the development of major chronic diseases like atherosclerosis,



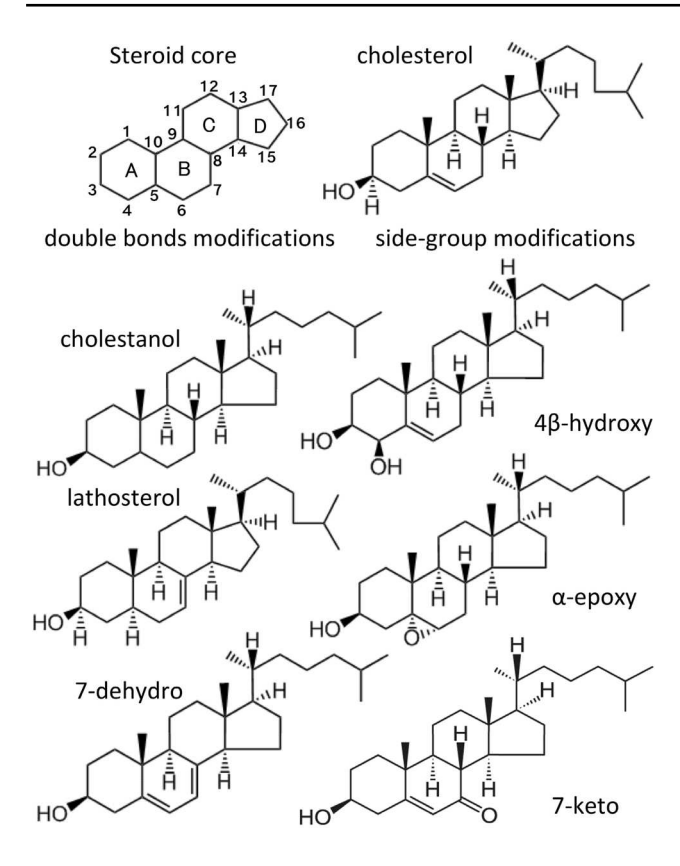


Fig. 1 Top Left: Nomenclature of the tetracyclic steroid core. Steroids considered in this study starting with cholesterol, top right, and two groups of sterols with modifications. The groups on the left have none, one, or two double bonds on the second steroid ring (**B**). The groups on the right—oxysterols—have side-group modifications in either the first (**A**) or second (**B**) steroid rings. In the figure, 7-dehydrocholesterol, 4β-hydroxycholesterol, 5α , 6α -epoxycholesterol, and 7-ketocholesterol are labeled: 7-dehydro, 4β-hydroxy, α -epoxy and 7-keto, respectively

neurodegenerative diseases, inflammatory bowel diseases, age-related macular degeneration, and other pathological conditions (Wielkoszynski et al. 2020; Anderson et al. 2020; Zmyslowski and Szterk 2019). For example, 7-ketocholesterol and other oxysterols, delivered into epithelial cells through oxy-LDL particles, are found to produce a loss of PM order leading to cell stiffening (Shentu et al. 2010, 2012).

Materials and Methods

Materials

1-palmitoyl(d31)-2-oleoyl-sn-glycero-3-phosphocholine (No 860399), cholesterol (source: ovine, No. 700000), lathosterol (5α -cholest-7-en-3 β -ol, No. 700069), 7-dehydrocholesterol (Δ 5,7-cholesterol, No. 700066), cholestanol (5α -cholestan-3 β -ol, No. 700064), 4 β -hydroxycholesterol

(cholest-5-ene-3ß,4ß-diol, No.700036), 5α ,6 α -epoxycholesterol (No.700032), and 7-ketocholesterol (3ß-hydroxy-5-cholestene-7-one, No.700015) were purchased, in powder form, from Avanti Polar Lipids (Alabaster, AL). D_2O was obtained from Cambridge Isotopes with 99.8% purity. Milli Q water (18 Ω) was obtained from a Millipore purification system available to users at neutron facilities.

Preparation of Unilamellar Lipid Vesicles

The phospholipid and sterols were mixed at a fixed molar ratio of 65:35 as dry powders. Sterol incorporation into membranes is limited, however. While POPC membranes can incorporate significant cholesterol (up to 61 mol% (Garg et al. 2014)), sterols that vary in the number and location of double bonds have been found to have lower limits (~40 mol% (Sheng et al. 2012; Stevens et al. 2010)). On the other hand, many oxysterols—and all those included in this study-have been found to incorporate into phospholipid membranes to at least ~ 50 mol% (Benesch and McElhaney 2016). Notwithstanding, there are oxysterols, like 25-hydroxycholesterol, that have very low solubility limits too (~15 mol%) (Benesch and McElhaney 2016). Hence, the choice of 65:35 for POPC:sterol was within the solubility range for all sterols in this study. Finally, in addition to being physiologically relevant, we found that in POPC, there is no effect on the transfer kinetics of cholesterol in the 20–40 mol% range (Perez-Salas et al. 2021).

The dry powder mixture of POPC/sterol was then dissolved in chloroform to ensure their proper mixing. Chloroform was removed by a flow of nitrogen followed by vacuum overnight at 60 °C. These mixtures were hydrated with solvents made of the appropriate ratio of D₂O and H₂O that achieve the correct neutron contrast match point for 1-palmitoyl(d31)-2-oleoyl-sn-glycero-3-phosphocholine (dPOPC)) (see SANS Contrast Matching section below). These aqueous suspensions were extruded through polycarbonate filters to produce small unilamellar vesicles with a diameter between 50 and 100 nm. As we reported recently, we found the exchange rates of cholesterol in 50 nm and 100 nm in POPC membranes to be similar (Perez-Salas et al. 2021). The stability of the vesicles was verified from the stability of the small-angle neutron scattering (SANS) patterns through the course of a few days during the experiments. Cholesterol is not known to form cholesterol-enriched domains in POPC while in the fluid phase up to its solubility limit of $\sim 61\%$ (Garg et al. 2014).

Small-Angle Scattering (SANS)

SANS measurements were performed on the NG3 30 m SANS instruments at the National Institute of Standards



and Technology Center for Neutron Research (NIST-CNR), Gaithersburg, MD and on D22 at the Institut Laue Langevin (ILL) in Grenoble, France.For the time-resolved kinetic measurements (TR-SANS), a single instrument configuration was used covering a Q-range of $0.003 < Q < 0.025 \, \text{Å}^{-1}$. Here, Q is the magnitude of the scattering vector given by $Q = 4\pi \sin(\theta/2)/\lambda$, where θ is the scattering angle and λ is the neutron wavelength. The wavelength used was $6 \, \text{Å}$ and the wavelength spread, $\Delta \lambda/\lambda$, was 30% at NIST and 10% at the ILL producing a higher intensity allowing for short time acquisition steps. Data were collected using a 2-D detector and reduced using the reduction package GRASP (Dewhurst and GRASP 2007). The reduced intensities were integrated over the whole detector and analyzed as a normalized total intensity as a function of time.

SANS Contrast Matching

One key aspect of these kinetic studies was to capture a scattering signal that is <u>only</u> due to the sterols. To do this, we rendered the phospholipids in the vesicles invisible by having their scattering length density (SLD) be matched to that of the solvent, a mixture of D_2O and H_2O . Deuterium-substituted hydrogen in the tails of the phospholipids or in the water render these isotopes very different neutron scattering cross sections than the fully hydrogenated species. For example, H_2O has a $SLD = -0.510-6 \ {\rm A}^{-2}$, while for D_2O , it is $6.33-6 \ {\rm A}^{-2}$ and mixtures of the two give a spectrum of SLD values in between. The proper ratio required to match the SLD of dPOPC is determined by measuring the SANS intensity from these vesicles in varying mixtures of D_2O and H_2O . The intensity produced by non-interacting vesicles is given by

$$I(Q) - I_{\text{background}} = v \left(\text{SLD}_{\text{vesicle}} - \text{SLD}_{\text{solvent}} \right)^2 P(Q)_{\text{vesicle,}}$$
(1)

where $P(Q)_{\rm vesicle}$ is the form factor of the vesicle, v is the volume fraction of vesicles, and $I_{\rm background}$ corresponds to the background signal. The contrast match point (point at which the SLD difference between the vesicles and solvent equals zero) is obtained by plotting the square root of the low Q intensity versus the volume fraction of D_2O (or H_2O). For dPOPC, the match point was found to be at a volume fraction of 48.6% D_2O (Garg et al. 2011). Therefore, all experiments in this study were performed in 48.6% D_2O .

Sterol Transfer Measurements

As described previously (Perez-Salas et al. 2021), sterol transfer rates are obtained by preparing two vesicle populations, the donor vesicles, consisting of dPOPC and the sterol, and the acceptor vesicles, consisting of only dPOPC. Both donor

and acceptor vesicle populations were prepared using the 48.6 volume % D_2O solvent to contrast match the phospholipids. At t=0, donor and acceptor vesicle solutions were mixed, and SANS intensity patterns are measured as a function of time. In this case, the scattering spectra have two contributions: donor and acceptor vesicles and given by

$$I(Q) - I_{\text{incoh}} = v_d \left(\text{SLD}_d - \text{SLD}_{\text{solvent}} \right)^2 P(Q)_d + v_a \left(\text{SLD}_a - \text{SLD}_{\text{solvent}} \right)^2 P(Q)_a$$
(2)

This expression simplifies when we incorporate the fact that the phospholipids are contrast matched and that initially the sterols are in the donor vesicles (Perez-Salas et al. 2021; Breidigan et al. 2017):

$$I(Q,t) = \beta(Q)\tilde{I}(t), \tag{3}$$

where $\beta(Q)$ is the time-independent factor given by

$$\beta(Q) = v_d \Delta \text{SLD}^2 \phi_d^2(0) P(Q), \tag{4}$$

where $\Delta \text{SLD} = \text{SLD}_{\text{sterol}} - \text{SLD}_{\text{membrane}}, P(Q)$ is the form factor for the vesicles, v_d is the volume fraction of donor vesicles, and $\phi_d(0)$ is the concentration of the sterol in the donor vesicles at t=0.

 $\tilde{I}(t)$ is the normalized total intensity and describes the sterol compositional changes in both the donor and acceptor vesicles as a result of the transfer of only the sterols and given by

$$\tilde{I}(t) = \varphi_d^2(t) + \frac{v_d}{v_a} \left(1 - \varphi_d(t)\right)^2,\tag{5}$$

where $\varphi_d(t) = \varphi_d(t)/\varphi_d(0)$ and v_a is the volume fraction of acceptor vesicles. Thus $\tilde{I}=1$, which reflects that, initially, the acceptor vesicles are devoid of sterols. At $t\to\infty$, if $v_d=v_a$, then $\varphi_d=1/2$ which in turn results in $\tilde{I}=1/2$, meaning an overall intensity drop by half at equilibrium. Experimentally, each time point corresponds to a scattered intensity corrected for solvent scattering (by subtracting the scattering from pure solvent) and integrated over the Q-range of $0.003 < Q < 0.025 \ {\rm \mathring{A}}^{-1}$ and normalized according to the initial (t=0) state.

Obtaining Kinetic Sterol Transfer Rates

The time-dependent sterol compositional changes in donor and acceptor vesicle populations are determined by the exchange rate of sterols, k_{ex} , through the solvent *between vesicle populations*, and flip-flop rates, k_f , of the movement of sterols *between inner and outer membrane leaflets* and are described by four coupled differential equations:

$$\frac{d\varphi(t)_{\text{in_}d}}{dt} = -k_f \left(\varphi(t)_{\text{in_}d} - \varphi(t)_{\text{out_}d} \right)$$
 (6a)



$$\frac{d\varphi(t)_{\text{out_}d}}{dt} = k_f \left(\varphi(t)_{\text{in_}d} - \varphi(t)_{\text{out_}d} \right) - k_{ex} \varphi(t)_{\text{out_}d} + k_{ex} \varphi(t)_{\text{out_}a}$$
(6b)

$$\frac{d\varphi(t)_{\text{out_}a}}{dt} = k_f \left(\varphi(t)_{\text{in_}a} - \varphi(t)_{\text{out_}a} \right) - k_{ex} \varphi(t)_{\text{out_}a} + k_{ex} \varphi(t)_{\text{out_}d}$$
(6c)

$$\frac{d\varphi(t)_{\text{in}_a}}{dt} = -k_f \left(\varphi(t)_{\text{in}_a} - \varphi(t)_{\text{out}_a} \right)$$
 (6d)

where the indices d and a refer to donor and acceptor populations, and out and in refer to the inner and outer leaflets. Here, $\varphi_d = \varphi(t)_{\text{in_}d} + \varphi(t)_{\text{out_}d}$, and thus, from the solution of Eqs. 6., the normalized total intensity (Eq. 5) can be directly compared to the data to obtain the exchange and flip-flop rates.

Equations 6 reflect the case where both populations are of equal size (in concentration and the size of the vesicles) as well as the assumption that the inner and outer leaflet volumes are equal. If the donor and acceptor populations are unequal, a slight modification to Eqs. 6. has to be made, as shown by Perez-Salas et al. (2021), but where ultimately the exchange rates can be recast to k_{ex} for equal populations; this then allows for rate comparisons between different population ratios.

Results

As mentioned in the introduction, we were interested in systematically exploring the transfer characteristics of sterols between and within membranes that differ from cholesterol by the number of double bonds in the second steroid ring (ring B, as shown in Fig. 1) as well as derivatives of cholesterol obtained by oxidation, specifically, hydroxyl, epoxy, and ketone side-group modifications in both the first and second rings, A and B, as shown in Fig. 1. Figure 1 shows the sterols included in this study.

As described in the Methods, with TR-SANS, we follow the transfer of sterol molecules through the aqueous environment from donor vesicles to acceptor vesicles by measuring the intensity changes resulting from the changes in sterol composition in the vesicles. Figure 2A shows the time-dependent total normalized intensity curves resulting from the transfer of sterols that have different number of double bonds in the second (B) steroid ring: 7-dehydrocholesterol (two double bonds), cholesterol (one double bond), lathosterol (one double bond), and cholestanol (no double bonds). Total normalized intensity curves in the figure were also captured for experiments done at different temperatures. Figure 2B compares the intensity decay curves for these four sterols at 60 °C. At this temperature, we see that cholestanol, which has no double bonds in its structure, exchanges slower than the sterols that have one or two double bonds in the second steroid ring (B). Sterols with one or two double bonds have, in contrast, similar transfer characteristics at 60 °C, particularly their movement between vesicles, which we describe as an exchange process. Cholesterol stands out because it behaves similar to 7-dehydrocholesterol and lathosterol in the initial exchange process; however, it clearly displays a slowdown in the equilibrium process at later times. This, as we have shown previously (Perez-Salas et al. 2021), is indicative of a second slower process which we identified to be flip-flop, the movement of the sterol across inner and outer leaflets within a membrane. In contrast, 7-dehydrocholesterol and lathosterol continue their fast homogenization, indicative of faster flip-flop—relative to the exchange process. Kinetic exchange rates (and flip-flop, if slower or comparable to the exchange process) were obtained from fits to normalized intensity curves, shown in Fig. 2A and B, using Eq. 5 and the time-dependent sterol concentration in the outer and inner leaflets of donor and acceptor populations as described by Eqs. 6. Figure 2C shows the kinetic exchange rates plotted against their temperature dependence. In this plot, we can observe that the exchange rates do follow a trend in which the number of double bonds affects how fast the exchange process occurs, following a sequence consistent with the number of double bonds in ring B. That is, in the temperature range studied, cholestanol is the slowest followed by cholesterol and lathosterol which have similar rates, and finally, 7-hydrocholesterol which is the fastest. In this plot, we are also able to capture trends in the activation energy for the exchange process (which follow or assume to follow an Arrhenius behavior). We find that for 7-dehydrocholesterol with two double bonds in ring B, the activation energy is slightly lower compared to the activation energy of cholesterol, cholestanol, and lathosterol. Because the latter sterols were measured for only two temperatures, they provide a trend (assuming an Arrhenius behavior) rather than a suitable quantitative comparison. Nonetheless, it can certainly be discerned from these data that as the number of double bonds increases in ring B the exchange rates become faster. Further, there is a lower activation energy for the exchange process for sterols that have two double bonds in ring B compared to one or none.

Being able to detect flip-flop is directly connected to the exchange rate: if the flip-flop rate is faster than the exchange process (by more than a factor ~ 1.5 (Perez-Salas et al. 2021)), then it is not possible to discern the flip-flop process with TR-SANS. As shown in Fig. 2A and B, we found that for cholestanol, lathosterol, and 7-dehydrocholesterol, the flipping rates are faster than the exchange rates, in contrast to cholesterol where the flipping rates are slower than the exchange rates.

In addition to double bonds in the steroid ring B, we studied changes in the transfer rates due to side-group



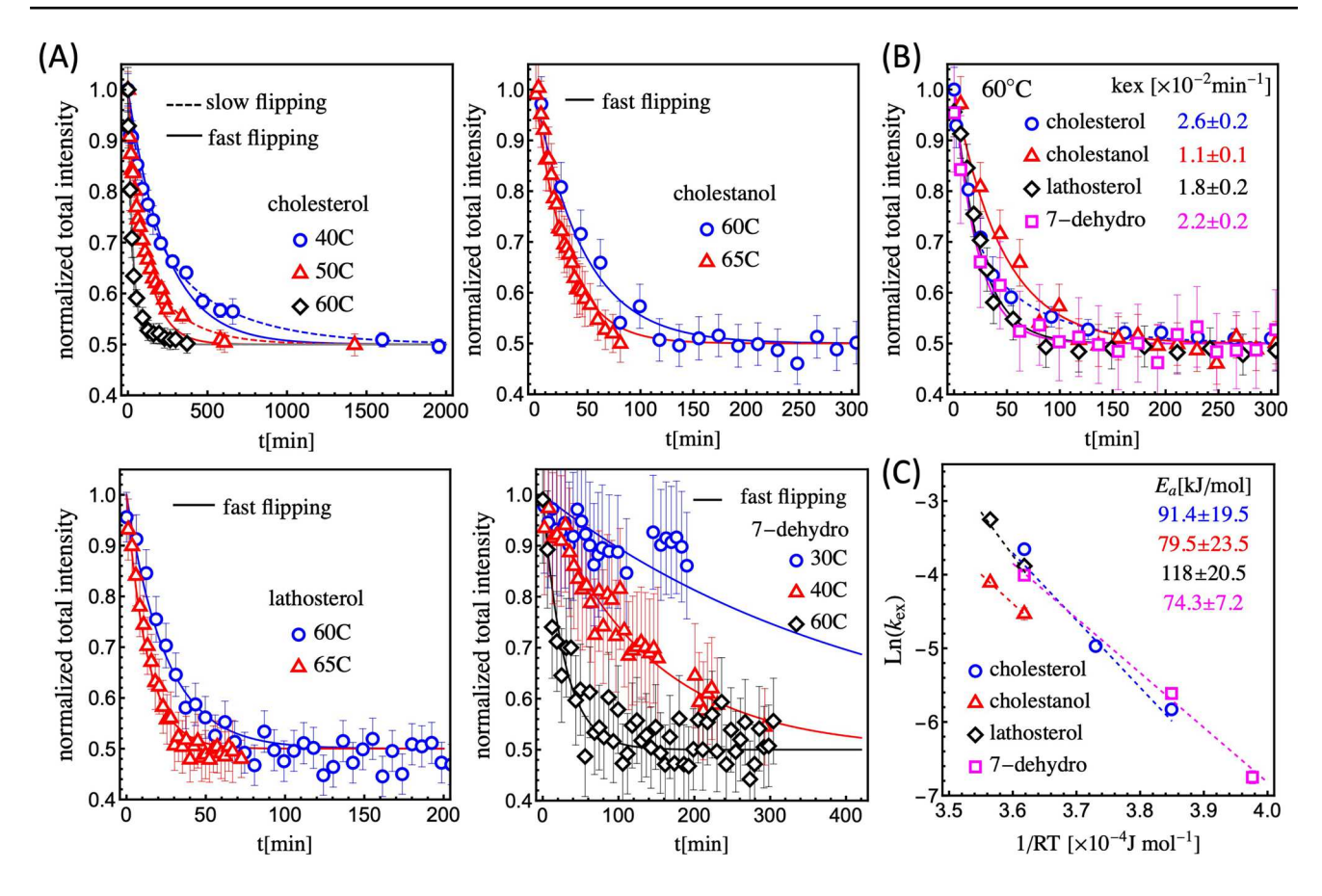


Fig. 2 A Normalized intensity as a function of time for two or three temperatures, with corresponding fits using Eqs. 5 and 6, showing the temperature dependence of transport kinetics in ~100 nm dPOPC vesicles. **B** Comparison of the normalized total intensity at 60 °C between sterols varying in the number of double bonds in the steroid ring B (see Fig. 1). **C** Arrhenius fits for exchange rates for the sterols shown in (A). Error bars for the rates correspond to the S.E. to

fits using Eqs. 5 and 6. Error bars are smaller than the symbols used. Error bars to the activation energy correspond to the S.E. to linear fits to the rates as a function of temperature. In the case of cholestanol and lathosterol, having only two points, a manual estimate of the activation energy error was done using the corresponding error in the rates. All fits to the data were weighted for their uncertainty

modifications belonging to oxysterols. Figure 3A shows the normalized total intensity for sterols with a side-group modification in either ring A: 4β -hydroxy or ring B: α -epoxy and 7-keto at several temperatures. Figure 3B compares the normalized total intensity for these sterols and in contrast to cholesterol at 40 °C (7-keto at 37 °C) showing that the transfer of these sterols through the aqueous medium is significantly faster than cholesterol. Fits with Eqs. 5 and 6 found that the flip-flop rates were inaccessible in these TR-SANS measurements, indicating that this process is faster than the exchange rate, in contrast to cholesterol, where such distinction can be made. Differences between the sterols are highlighted in Fig. 3C, where the rates obtained through fits using Eqs. 5 and 6 are plotted against temperature. Comparing the exchange rates of these oxysterols we find that, sequentially, 4β-hydroxy has the slowest rates, while 7-keto has the fastest, with α -epoxy in between. Therefore, from these data, one can conclude that oxysterols with a side-modification in ring B produce faster exchange rates than side-group modifications in ring A.

The energetics of the exchange rates can be extracted from the Arrhenius behavior of the rates with temperature as shown in Fig. 3C. Interestingly, the activation energy for exchange follows a clear trend showing a consistent decrease in the activation energy starting with the highest activation energy for cholesterol (91.4 \pm 13.2 kJ/mol) to 4 β -hydroxy (69.0 \pm 13 kJ/mol) to α -epoxy (65.5 \pm 15 kJ/mol) to 7-keto (53.8 \pm 1.6 kJ/mol) which has the lowest energy of activation of the sterols studied.

An important check during the in situ measurement of the exchange of sterols between vesicles is to verify that their shape and size remain constant over the duration of the experiment. Figure 4 shows the scattering curves for the transfer of 7-keto cholesterol between vesicles at 37 °C. A fit of the scattering data at t=0 provides the vesicles size, composition, and vesicle concentration of the donor vesicles



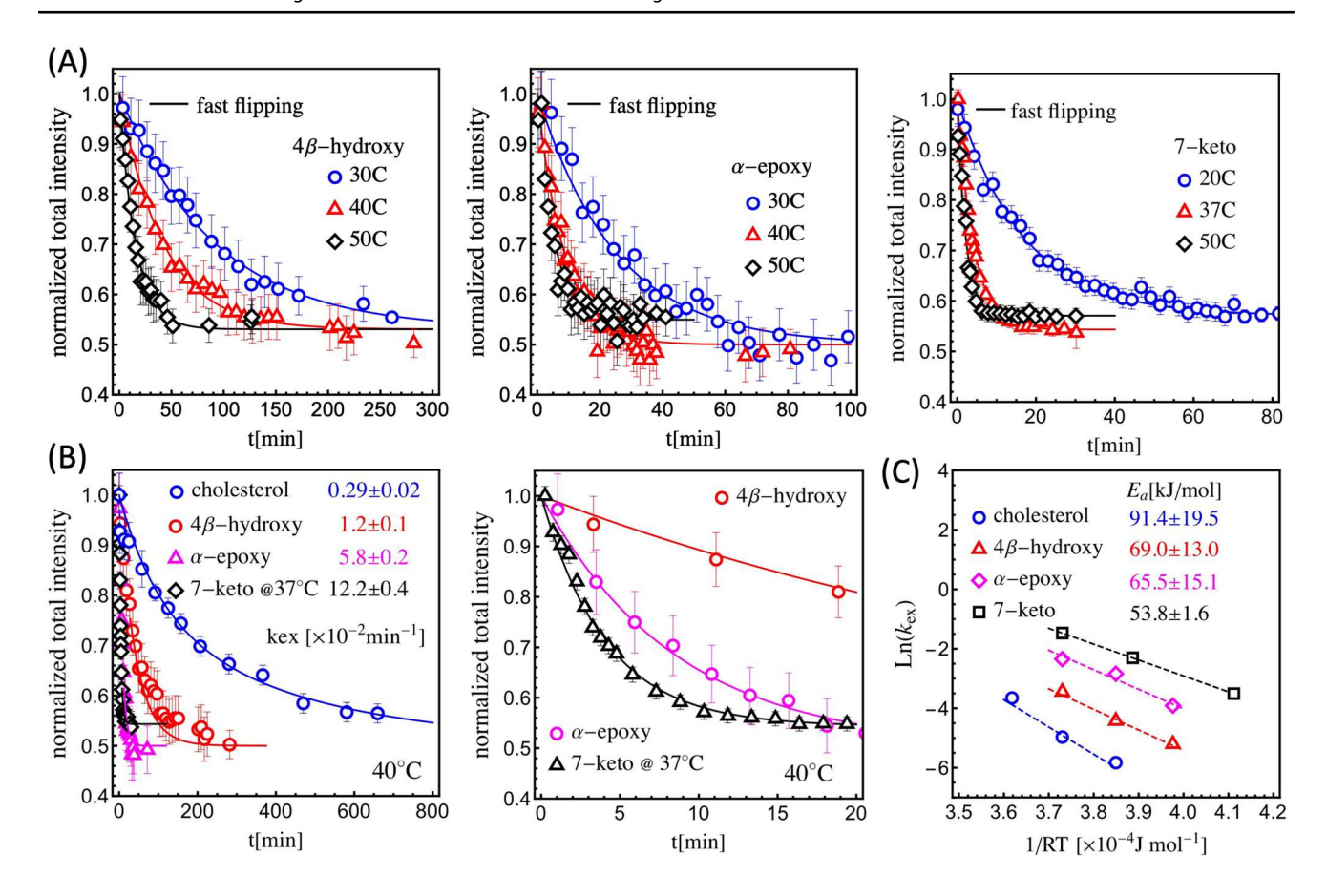


Fig. 3 A Normalized intensity as a function of time for three temperatures, with corresponding fits, showing the temperature dependence of transport kinetics in ~100 nm dPOPC vesicles for oxysterols 4β-hydroxy, α-epoxy, and 7-keto (see Fig. 1). **B** Comparison of the normalized total intensity at 40 °C between cholesterol and oxysterols with side-modifications in ring A (4β-hydroxy) and ring B (α-epoxy and 7-keto); plot on the right shows a comparison for the change in normalized intensity for oxysterols only during the initial exchange

process highlighting the differences between α -epoxy and 7-keto and these compared to 4β -hydroxy. C Arrhenius fits for the exchange rates found the sterols shown in (A) and cholesterol, (shown in Fig. 2C). Error bars for the rates correspond to the S.E. to fits using Eqs. 5 and 6. Error bars to the activation energy correspond to the S.E. to linear fits to the rates as a function of temperature. Error bars of the rates are smaller than the symbols used. All fits to the data were weighted for their uncertainty

(Eq. 4), which also serves as a check of the known vesicle preparation conditions. As described in Eq. 3, the time evolution of the scattering curves is obtained using the prefactor $\tilde{I}(t)$ which, in Fig. 4, is shown to be consistent with the data.

Known characteristics of these sterols can shed light into their ability to desorb from membranes, a process we have referred to as exchange. Parameters like Log P, where P is the compound's partitioning coefficient between n-octanol and water, and Log S, where S is the solubility of a compound in water, have been widely used to correlate solute partitioning phenomena and absorption (Savjani et al. 2012). Structure parameters, like the topological polar surface area (TPSA), which is related to the accessibility of a molecule to aqueous solvents through its polar groups, have been useful in computational modeling to reveal relationships between structural properties of chemical compounds and

their pharmacological or biological activity (Prasanna and Doerksen 2009). Figure S1 and S2 in the supplementary information shows the exchange rates at 50 °C (S1), as well as the activation energy (S2), against Log P, Log S, and TPSA for all sterols studied shown in Fig. 1. In these figures, 4β-hydroxy was found to be somewhat inconsistent with the trends displayed by the other sterols, particularly against Log P and TPSA. In order to understand this discrepancy, we plotted Log P versus Log S, which should display a linear relation as shown by Miller et al. (and other authors referenced therein) (Miller et al. 1985). Indeed, all sterols, except 4ß-hydroxy, follow this free energy-derived linear relation (see figure S3) and therefore was excluded from the following analysis. Figure 5 shows the exchange rates at 50 °C against LogP, LogS and TPSA. In all the plots, we see that the rates increase as the partitioning to water increases, or the solubility into water increases or the accessible polar



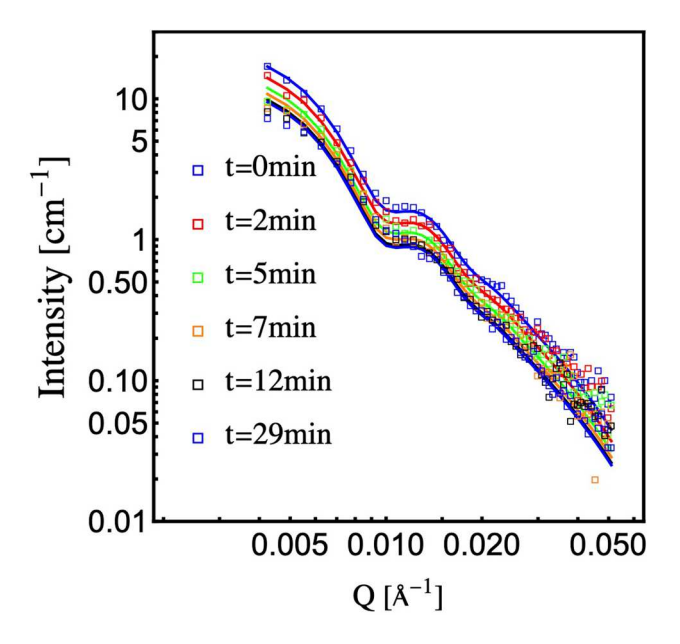


Fig. 4 Select scattering intensity curves versus the momentum transfer Q corresponding to the transfer of 7-keto between vesicles at 37 °C. The t=0 line corresponds to scattering from only donor vesicles. The lines through the data correspond to the evolution of the t=0 form factor according to the normalized intensity $\tilde{I}(t)$ shown in Fig. 3 and expressed in Eq. 3. The scattering curves between 12 and 29 min are nearly identical because the transfer of 7-keto has reached equilibrium. The t=0 fit (using the vesicle form factor in SASview (Doucet et al. 2021)) corresponds to vesicles having a 60 nm diameter, a bilayer thickness of 4 nm, a sterol concentration of 35 mol% in the vesicle membrane, and an overall lipid concentration of 10 mg/ml

area increases. The manner in which this happens for Log P and Log S, however, is marked by two regimes: one of slow rates (with less partitioning into water and less water solubility) and one of fast rates (having more partitioning into water and being more soluble in water) which coincides as well with the two distinct types of modification in the current study as described in Fig. 1. The regimes do display

continuity albeit the sharp change in the rates behavior with either Log P or Log S as shown in Fig. 5A and B. In contrast, as shown in Fig. 5C, these rates plotted against the structural parameter TRSA behave linearly. However, the lack of structural differences (as given by TPSA) for sterols having slow rates—i.e., all collapsing into one value of TPSA shows that this parameter has less sensitivity for differences between the exchange rates of these sterols. Figure 6 shows a consistent linear behavior for the activation energy when plotted against Log P, Log S, and TPSA. In these plots, cholestanol and lathosterol were excluded because the energetics obtained were based on only 2 points. As with the rates, we observe a lowering of the activation energy with an increase in water partitioning, as well as increased water solubility or increased access to the polar environment at the headgroup/solvent interface.

Because in these comparisons 4ß-hydroxy was excluded, we searched for a new parameter that would allow us to revisit this sterol. Atkovska et al. (2018) found that the partition coefficient, Log P, measured between water and n-octanol is in fact different from a partition coefficient obtained between water and a lipid environment. Indeed, membrane desorption rates require overcoming the free energy of membrane/water partitioning. Finer modulations to this free energy depend on a combination of determinants, including configurational flexibility (tilt and tilt distribution) and specific steroid - lipid interactions (such as its position along the membrane normal), in addition to the overall hydrophobicity of the molecule as given by Log P. The tilt and tilt distribution of sterols in membranes, characterized by the tilt modulus, has been identified as important to characterize other membrane characteristics as well, such as the bending rigidity of membranes, or as a useful tool to characterize the condensing effect of sterols on phospholipids (Khelashvili and Harries 2013a, 2013b). Figure 7 compares the tilt modulus for cholesterol, 4ß-hydroxy, and 7-keto in POPC membranes obtained at 37 °C by Kulig et al.

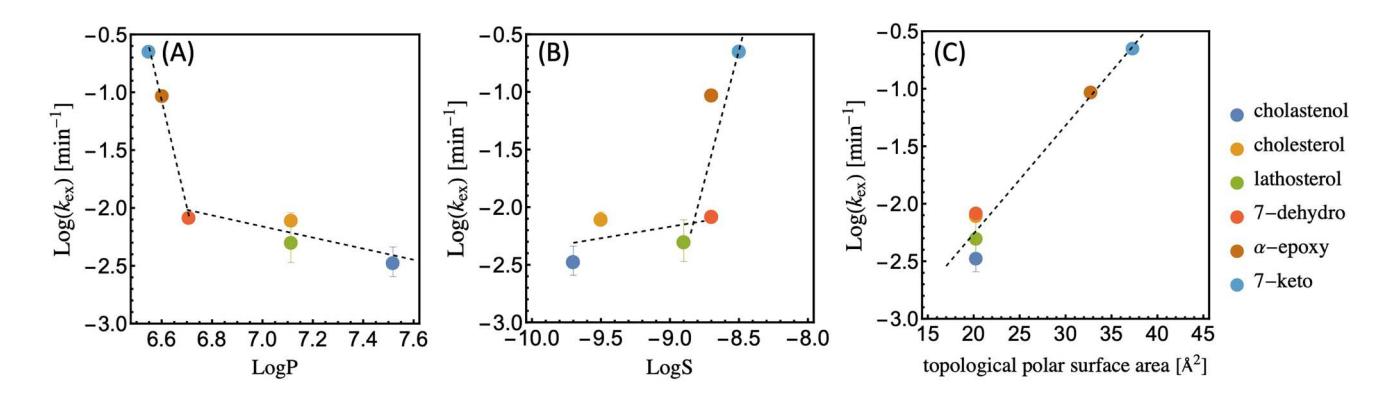


Fig. 5 Exchange rates at 50 °C (Figs. 2, 3) as a function of LogP (**A**), LogS (**B**), and topological polar surface area (TPSA) (**C**). Dashed lines are linear fits but are meant to serve as visual guides only.

The rates for cholestanol, lathosterol, and 7-dehydro at 50 $^{\circ}\mathrm{C}$ were obtained from the activation energy fits



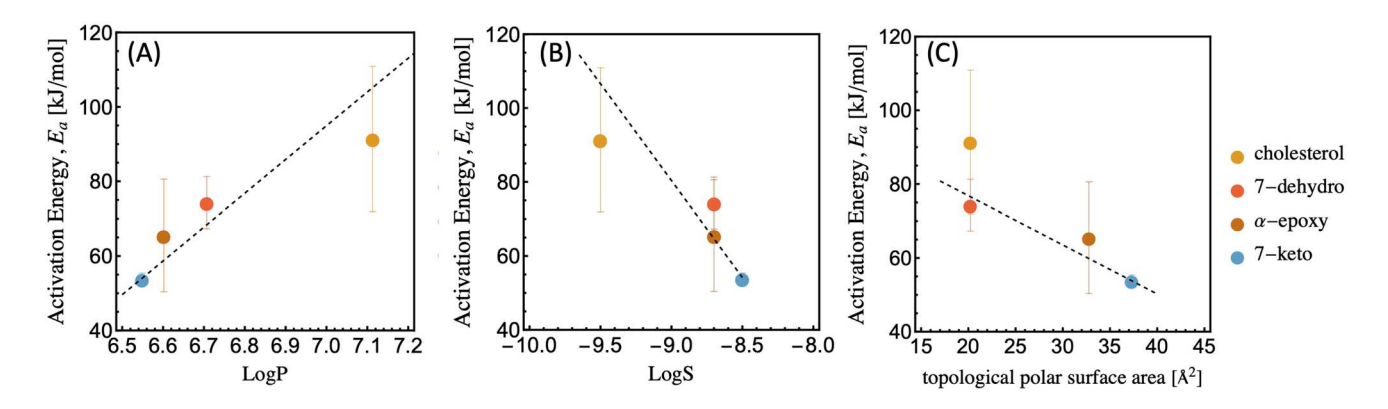


Fig. 6 Activation energies (Figs. 2C, 3C) as a function of LogP (A), LogS (B), and topological polar surface area (TPSA) (C). Because the energetics of cholestanol and lathosterol were obtained with only 2 points they were not included in these plots. Error bars are S.E.

to linear fits to the rates as a function of temperature, as shown in Figs. 2C and 3C. Dashed lines are linear fits but are meant to serve as visual guides only

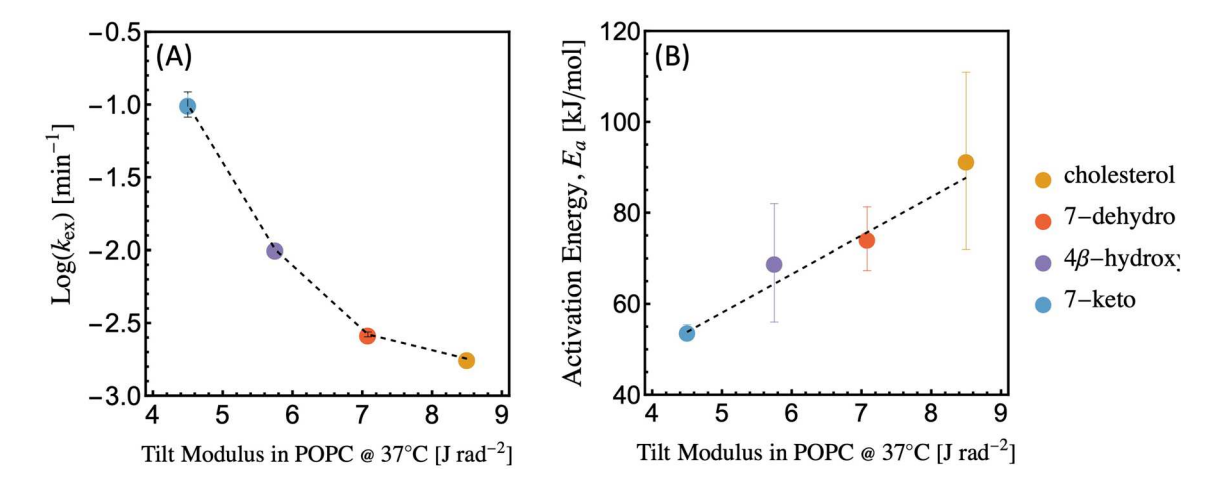


Fig. 7 Rates at 37 $^{\circ}$ C (A) and activation energy (B) as a function of the tilt modulus. The dash line is a visual aid only. The values of the tilt modulus are taken from Kulig et al. (2015)

(2015) to membrane desorption rates at 37 °C and activation energies obtained using TR-SANS for these sterols. Figure 7 also shows an estimated value for the tilt modulus for 7-dehydrocholesterol in POPC by comparing the relative behavior of the tilt modulus between cholesterol and 7-dehydrocholosterol in DMPC membranes (at 35 °C) obtained by Khelashvili et al. (2011) and extrapolating to the behavior of cholesterol in POPC membranes at 37 °C (Kulig et al. 2015). The larger values of the tilt modulus correspond to sterol requiring more (tilt) energy to move away from their preferred tilt configuration, while lower values of the tilt modulus correspond to sterols energetically able to span larger angular ranges. As shown in Fig. 7, we find that there is a clear correlation between the tilt modulus and the rates they increase, near-linearly, with decreasing tilt modulus. And, in contrast to Fig. 5A and B, the data appear to behave in a manner consistent with a single behavior, rather than having two regimes. As was the case in Fig. 6, the energetics appears to show a linear increasing trend against increasing tilt modulus. Figure 7, which now includes 4ß-hydroxy, suggests that indeed the tilt modulus is a good predictor to the energetics and rates of desorption and that the free energy of membrane/water partitioning is more reliable for lipid/water mixtures. Here, we just highlight that one way to obtain this free energy is through the potential of mean force (PMF) or experimentally using isothermal titration calorimetry (Samelo et al. 2017), for example.

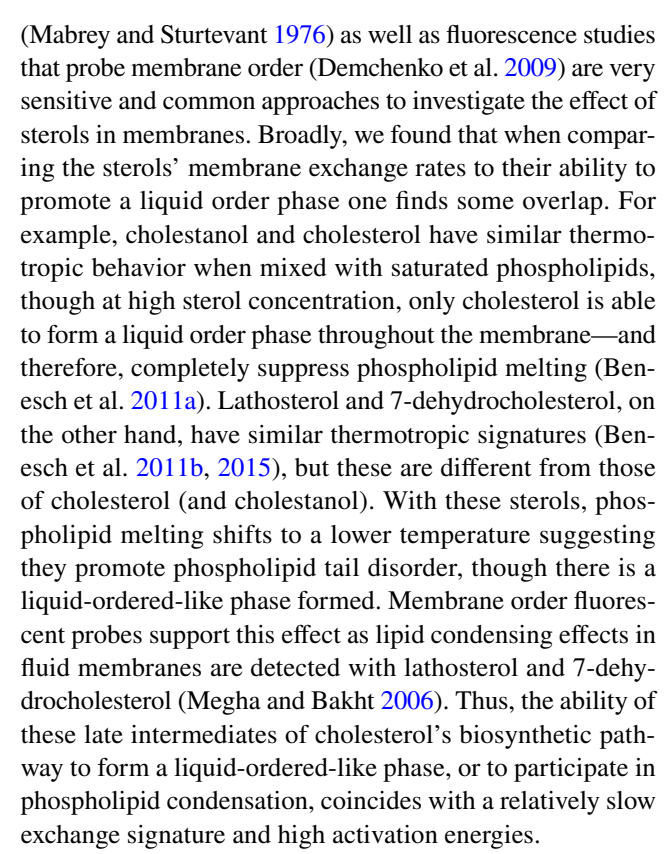
Discussion

Due to the low solubility of lipids in an aqueous environment, the view is that no significant lipid transport of biological impact can proceed between membranes. As a result, cells utilize transporters to do this work. The transport properties of lipids through an aqueous medium,



however, vary significantly, and therefore, their dependence on transporters to move between membranes must vary too. Atkovska et al. (2018), using MD simulations, found large variations in the exiting rates of steroid molecules from membranes, from 10^{-5} to 10^4 s (~9 orders of magnitude) depending on the sterol's structure. When the steroids had a long cholesterol-like hydrophobic tail at C17 of the steroid core, the exit rates from the membrane were the slowest, varying between $\sim 6 \times 10^{-2}$ and $6 \times 10^{-4} \text{ min}^{-1}$ (at 27 °C). However, these two orders of magnitude difference are significant, covering half-times of many hours to a few minutes. At 37 °C, we found that for sterols having no double bonds (cholestanol), or having one double bond, at either position C5–C6 (cholesterol) or at position C7–C8 (lathosterol), the exchange half-times were ~ 10 h, while with two double bonds, one at position C5-C6 and the other at C7-C8 (7-dehydrocholesterol), the exchange half-time decreased to 4 h. Structurally, 7-dehydrocholesterol's steroid core has a clear twist due to the two double bonds, and therefore lose the consistent flat configuration of the steroid core found in cholestanol, cholesterol, and lathosterol. Even though these sterols exchange slowly between membranes, they are about ~ 20 times faster than what we have found for long tail phospholipids, like POPC (Perez-Salas et al. 2021). Oxidized modifications produce even faster half-times; a side-group modification in ring A (4β-hydroxy) produced a half-time of ~ 1 h, while side-group oxygen modifications in ring B (α -epoxy and 7-keto) give half-times in minutes: 20 and 7 min, respectively. For these sterols, the steroid core remains flat, having one (4β-hydroxy and 7-keto) or no double bonds (α -epoxy); however, the oxidized modifications produce a tendency to change the tilt away from the membrane normal and move them closer to the headgroup region of the membrane (Kulig et al. 2015; Massey and Pownall 2005). Further, these oxidized sterols have a lower tilt modulus compared to those just varying in number of double bonds, as shown in Fig. 7, giving the sterols more freedom within the membrane. Structurally, 4β-hydroxy not only becomes more hydrophilic with the addition of an OH group in ring A and therefore more proximal to the headgroup region, but its location at C4 suggests that it facilitates a slight tilt change away from the normal (Kulig et al. 2015). An oxygen modification on ring B on either the smooth face (α -epoxy) or rough face (7-keto) of the steroid core also suggests that it facilitates a tilt shift away from the membrane normal and a tendency for this oxygen to approach the headgroup region of the membrane (Massey and Pownall 2005).

An important additional characteristic studied when investigating sterols is their effect on membrane order and the formation of lipid rafts (Brown and London 1998a, 1998b). Thermotropic studies of lipids using calorimetry



The presence of hydroxy, keto, or epoxy groups on the steroid ring system (A or B steroid rings in this case) reduces the temperature and cooperativity in the melting transition of saturated phospholipids as well, indicating that their presence thermally destabilizes order in the membrane which is similar to that observed for lathosterol and 7-dehydrocholesterol, but having more pronounced disordering effects (Benesch and McElhaney 2016). Membrane order fluorescent probes support this effect as well, where, for example, 7-keto is found to maintain liquid-ordered domains though not as tightly packed as those formed with cholesterol (Wang and Megha 2004) or directly on cells where the oxysterols (such as 7-keto) produced, consistently though in varying degrees, less order in membranes compared to cholesterol (Shentu et al. 2010, 2012). The increased disruption of membrane order is consistent with a highly mobile environment for the sterols, and this is consistent with higher rates of membrane desorption and a lower activation energy.

Conclusion

Lipids can a diffuse through the aqueous environment, but the relative ease with which this happens can vary by several orders of magnitude; at physiological temperatures, this can take many hours or a few minutes depending on their structural and behavioral characteristics in membranes. As a result, how these molecules are transported between different



membrane compartments in cells can vary significantly too. Hence, the transport of lipids between membranes is likely achieved by not only transporters and vesicles but may also be transported by passive diffusion.

Here, we found that double bonds on the steroid core corresponding to late precursors of cholesterol's synthesis pathways behave similarly to cholesterol not only in their properties to still promote membrane order but, as we reported here, also have a relatively small effect in their transport signatures between membranes compared to cholesterol. Notwithstanding, the signatures, though similar, follow the number of double bonds in ring B: none being the slowest and two being the fastest. Similarly, the activation energies for membrane desorption were found to be the same within error bars ($\sim 90 \pm 20 \text{ kJ/mol}$). Oxysterols, found to be clear disruptors of membrane order (Ayee and Levitan 2021; Shentu et al. 2010, 2012), were found to move significantly faster between membranes and the activation energy followed a sequential behavior, where faster desorption rates also corresponded to lower activation energies. Both the rates and energetics correlated with the partitioning coefficient (Log P) and solubility (Log S) except for 4ß-hydroxy. Interestingly, we found that the tilt modulus, which reflects the sterol's preferred tilt and the tilt's distribution, was highly correlated with the desorption rates and energetic characteristics of these sterols, including 4ß-hydroxy. Hence, we found that the tilt modulus is a better predictor of how fast sterols desorb from membranes and thus exchange with other membranes. In the case of oxysterols, the tilt modulus reflects a most probable tilt angle that is further away from the membrane normal than cholesterol's (or sterols having different degrees of saturation in ring B) and also having a high degree of angular mobility (a broad angular distribution) within the membrane, which is clearly facilitating their exit into the aqueous environment. Oxysterols are typically stored in oxidized low density lipoprotein (oxy-LDL) particles which, when endocytosed by cells, produce both cell stiffening and membrane disorder (Ayee and Levitan 2021; Shentu et al. 2010, 2012). However, as we show here, oxysterols can move with relative ease through the aqueous environment and therefore may affect the cell's plasma membrane even prior to being internalized. Hence, connecting this type of fast but passive transport behavior to the larger network of transporters of sterols (Shentu et al. 2010) could be an important contribution to understanding membrane physiology under oxidative conditions (Dittman and Menon 2017).

Supplementary Information The online version contains supplementary material available at https://doi.org/10.1007/s00232-022-00231-3.

Acknowledgements This work utilized the facilities at the National Institute for Standards and Technology, supported in part by the National Science Foundation under agreement no. DMR-0454672. Commercial materials or equipment if identified in this paper do not imply recommendation or endorsement by the National Institute of Standards and Technology nor should be identified as the best available for the purpose. The authors thank the Institute Laue Langevin for providing neutron beam time under https://doi.org/10.5291/ILL-DATA.9-13-823. U.P.-S. additionally acknowledges travel support from the ILL to promote scientific collaboration with L. Porcar, Y. Gerelli, and G. Fragneto. U.P.-S. gratefully acknowledges the support from the NSF CAREER award DMR-1753238. IL gratefully acknowledges the support from NIH R01HL073965, R01HL141120, and R01HL083298.

Funding This study was funded by NSF, CAREER award DMR-1753238 (UPS) as well as supported by R01HL073965 (IL), R01HL141120 (IL), R01HL083298 (IL).

Data Availability The datasets analyzed during the current study are available from the corresponding author on reasonable request. All data generated or analyzed during this study are included in this published article and its supplementary information file.

Declarations

Conflict of interest Authors Perez-Salas, Porcar, Garg, Ayee and Levitan declare no conflict of interest.

Ethical Approval This article does not contain any studies with human participants or animals performed by any of the authors.

References

Anderson A, Campo A, Fulton E, Corwin A, Jerome WG III, O'Connor MS (2020) 7-Ketocholesterol in disease and aging. Redox Biol 29:101380

Atkovska K, Klingler J, Oberwinkler J, Keller S, Hub JS (2018) Rationalizing steroid interactions with lipid membranes: conformations partitioning, and kinetics. ACS Cent Sci 4(9):1155–1165

Ayee MAA, Levitan I (2021) Lipoprotein-induced increases in cholesterol and 7-ketocholesterol result in opposite molecular-scale biophysical effects on membrane structure. Front Cardiovasc Med 8:715932

Bacia K, Schwille P, Kurzchalia T (2005) Sterol structure determines the separation of phases and the curvature of the liquid-ordered phase in model membranes. Proc Natl Acad Sci USA 102(9):3272–3277

Benesch MG, McElhaney RN (2016) A comparative differential scanning calorimetry study of the effects of cholesterol and various oxysterols on the thermotropic phase behavior of dipalmitoylphosphatidylcholine bilayer membranes. Chem Phys Lipids 195:21–33

Benesch MG, Mannock DA, McElhaney RN (2011a) Sterol chemical configuration influences the thermotropic phase behaviour of dipalmitoylphosphatidylcholine bilayers containing 5alphacholestan-3beta- and 3alpha-ol. Chem Phys Lipids 164(1):62–69

Benesch MG, Mannock DA, Lewis RN, McElhaney RN (2011b) A calorimetric and spectroscopic comparison of the effects of lathosterol and cholesterol on the thermotropic phase behavior and organization of dipalmitoylphosphatidylcholine bilayer membranes. Biochemistry 50(46):9982–9997



- Benesch MG, Lewis RN, McElhaney RN (2015) A calorimetric and spectroscopic comparison of the effects of cholesterol and its immediate biosynthetic precursors 7-dehydrocholesterol and desmosterol on the thermotropic phase behavior and organization of dipalmitoylphosphatidylcholine bilayer membranes. Chem Phys Lipids 191:123–135
- Bernsdorff C, Winter R (2003) Differential properties of the sterols cholesterol, ergosterol, β-Sitosterol, trans-7-dehydrocholesterol Stigmasterol and Lanosterol on DPPC Bilayer Order. J Phys Chem B 107(38):10658–10664
- Bloch KE (1983) Sterol structure and membrane function. CRC Crit Rev Biochem 14(1):47–92
- Breidigan JM, Krzyzanowski N, Liu Y, Porcar L, Perez-Salas U (2017) Influence of the membrane environment on cholesterol transfer. J Lipid Res 58(12):2255–2263
- Brown DA, London E (1998a) Functions of lipid rafts in biological membranes. Annu Rev Cell Dev Biol 14:111–136
- Brown DA, London E (1998b) Structure and origin of ordered lipid domains in biological membranes. J Membr Biol 164(2):103–114
- Chiang JY (2004) Regulation of bile acid synthesis: pathways, nuclear receptors, and mechanisms. J Hepatol 40(3):539–551
- Delle Bovi RJ, Kim J, Suresh P, London E, Miller WT (2019) Sterol structure dependence of insulin receptor and insulin-like growth factor 1 receptor activation. Biochim Biophys Acta Biomembr 1861(4):819–826
- Demchenko AP, Mely Y, Duportail G, Klymchenko AS (2009) Monitoring biophysical properties of lipid membranes by environment-sensitive fluorescent probes. Biophys J 96(9):3461–3470
- Dewhurst (2007) GRASP: graphical reduction and analysis SANS program for Matlab. https://www.ill.eu/users/support-labs-infra structure/software-scientific-tools/grasp
- Dittman JS, Menon AK (2017) Speed limits for nonvesicular intracellular sterol transport. Trends Biochem Sci 42(2):90–97
- Doucet M, Cho JH, Alina G, Attala Z, Bakker J, Bouwman W, Butler PD, Campbell K, Cooper-Benun T, Durniak C, Forster L, Gonzalez M, Heenan R, Jackson A, King S, Kienzle P, Krzywon J, Murphy R, Nielsen T, O'Driscoll L, Potrzebowski W, Prescott S, Ferraz Leal R, Rozyczko P, Snow T, Washington A (2021) SASview
- Dufourc EJ (2008) Sterols and membrane dynamics. J Chem Biol 1(1-4):63-77
- Epand RM (2006) Cholesterol and the interaction of proteins with membrane domains. Prog Lipid Res 45(4):279–294
- Garg S, Porcar L, Woodka AC, Butler PD, Perez-Salas U (2011) Noninvasive neutron scattering measurements reveal slower cholesterol transport in model lipid membranes. Biophys J 101(2):370–377
- Garg S, Castro-Roman F, Porcar L, Butler P, Bautista PJ, Krzyzanowski N, Perez-Salas U (2014) Cholesterol solubility limit in lipid membranes probed by small angle neutron scattering and MD simulations. Soft Matter 10(46):9313–9317
- Hu J, Zhang Z, Shen WJ, Azhar S (2010) Cellular cholesterol delivery, intracellular processing and utilization for biosynthesis of steroid hormones. Nutr Metab (lond) 7:47
- Ikonen E, Zhou X (2021) Cholesterol transport between cellular membranes: a balancing act between interconnected lipid fluxes. Dev Cell 56(10):1430–1436
- Khelashvili G, Harries D (2013a) How cholesterol tilt modulates the mechanical properties of saturated and unsaturated lipid membranes. J Phys Chem B 117(8):2411–2421
- Khelashvili G, Harries D (2013b) How sterol tilt regulates properties and organization of lipid membranes and membrane insertions. Chem Phys Lipids 169:113–123
- Khelashvili G, Rappolt M, Chiu SW, Pabst G, Harries D (2011) Impact of sterol tilt on membrane bending rigidity in

- cholesterol and 7DHC-containing DMPC membranes. Soft Matter 7(21):10299–10312
- Krakowiak PA, Wassif CA, Kratz L, Cozma D, Kovarova M, Harris G, Grinberg A, Yang Y, Hunter AG, Tsokos M, Kelley RI, Porter FD (2003) Lathosterolosis: an inborn error of human and murine cholesterol synthesis due to lathosterol 5-desaturase deficiency. Hum Mol Genet 12(13):1631–1641
- Kulig W, Olzynska A, Jurkiewicz P, Kantola AM, Komulainen S, Manna M, Pourmousa M, Vazdar M, Cwiklik L, Rog T, Khelashvili G, Harries D, Telkki VV, Hof M, Vattulainen I, Jungwirth P (2015) Cholesterol under oxidative stress-How lipid membranes sense oxidation as cholesterol is being replaced by oxysterols. Free Radic Biol Med 84:30–41
- Lorent JH, Levental KR, Ganesan L, Rivera-Longsworth G, Sezgin E, Doktorova M, Lyman E, Levental I (2020) Plasma membranes are asymmetric in lipid unsaturation, packing and protein shape. Nat Chem Biol 16(6):644–652
- Lund R, Willner L, Stellbrink J, Lindner P, Richter D (2006) Logarithmic chain-exchange kinetics of diblock copolymer micelles. Phys Rev Lett 96(6):068302
- Mabrey S, Sturtevant JM (1976) Investigation of phase transitions of lipids and lipid mixtures by sensitivity differential scanning calorimetry. Proc Natl Acad Sci USA 73(11):3862–3866
- Massey JB, Pownall HJ (2005) The polar nature of 7-ketocholesterol determines its location within membrane domains and the kinetics of membrane microsolubilization by apolipoprotein A-I. Biochemistry 44(30):10423–10433
- Maxfield FR, Mondal M (2006) Sterol and lipid trafficking in mammalian cells. Biochem Soc Trans 34(Pt 3):335–339
- Maxfield FR, van Meer G (2010) Cholesterol, the central lipid of mammalian cells. Curr Opin Cell Biol 22(4):422–429
- McLean LR, Phillips MC (1981) Mechanism of cholesterol and phosphatidylcholine exchange or transfer between unilamellar vesicles. Biochemistry 20(10):2893–2900
- Megha O, Bakht E (2006) London, Cholesterol precursors stabilize ordinary and ceramide-rich ordered lipid domains (lipid rafts) to different degrees. Implications for the Bloch hypothesis and sterol biosynthesis disorders. J Biol Chem 281(31):21903–21913
- Menon AK (2018) Sterol gradients in cells. Curr Opin Cell Biol 53:37–43
- Miller MM, Wasik SP, Huang GL, Shiu WY, Mackay D (1985) Relationships between octanol-water partition coefficient and aqueous solubility. Environ Sci Technol 19(6):522–529
- Nakano M, Fukuda M, Kudo T, Endo H, Handa T (2007) Determination of interbilayer and transbilayer lipid transfers by time-resolved small-angle neutron scattering. Phys Rev Lett 98:238101
- Nes WD (2011) Biosynthesis of cholesterol and other sterols. Chem Rev 111(10):6423-6451
- Olkkonen VM, Beaslas O, Nissila E (2012) Oxysterols and their cellular effectors. Biomolecules 2(1):76–103
- Perez-Salas U, Garg S, Gerelli Y, Porcar L (2021) Deciphering lipid transfer between and within membranes with time-resolved small-angle neutron scattering. Curr Top Membr 88:359–412
- Phillips MC, Johnson WJ, Rothblat GH (1987) Mechanisms and consequences of cellular cholesterol exchange and transfer. Biochim Biophys Acta 906(2):223–276
- Porter FD (2002) Malformation syndromes due to inborn errors of cholesterol synthesis. J Clin Invest 110(6):715–724
- Prasanna S, Doerksen RJ (2009) Topological polar surface area: a useful descriptor in 2D-QSAR. Curr Med Chem 16(1):21–41
- Ripa I, Andreu S, Lopez-Guerrero JA, Bello-Morales R (2021) Membrane rafts: portals for viral entry. Front Microbiol 12:631274
- Samelo J, Mora MJ, Granero GE, Moreno MJ (2017) Partition of amphiphilic molecules to lipid bilayers by ITC: low-affinity solutes. ACS Omega 2(10):6863–6869



- Savjani KT, Gajjar AK, Savjani JK (2012) Drug solubility: importance and enhancement techniques. ISRN Pharm 2012:195727
- Serfis AB, Brancato S, Fliesler SJ (2001) Comparative behavior of sterols in phosphatidylcholine-sterol monolayer films. Biochim Biophys Acta 1511(2):341–348
- Shaghaghi M, Chen MT, Hsueh YW, Zuckermann MJ, Thewalt JL (2016) Effect of sterol structure on the physical properties of 1-palmitoyl-2-oleoyl-sn-glycero-3-phosphocholine membranes determined using (2)H nuclear magnetic resonance. Langmuir 32(30):7654–7663
- Sheng R, Chen Y, Yung Gee H, Stec E, Melowic HR, Blatner NR, Tun MP, Kim Y, Kallberg M, Fujiwara TK, Hye Hong J, Pyo Kim K, Lu H, Kusumi A, Goo Lee M, Cho W (2012) Cholesterol modulates cell signaling and protein networking by specifically interacting with PDZ domain-containing scaffold proteins. Nat Commun 3:1249
- Shentu TP, Titushkin I, Singh DK, Gooch KJ, Subbaiah PV, Cho M, Levitan I (2010) oxLDL-induced decrease in lipid order of membrane domains is inversely correlated with endothelial stiffness and network formation. Am J Physiol Cell Physiol 299(2):C218–C229
- Shentu TP, Singh DK, Oh MJ, Sun S, Sadaat L, Makino A, Mazzone T, Subbaiah PV, Cho M, Levitan I (2012) The role of oxysterols in control of endothelial stiffness. J Lipid Res 53(7):1348–1358
- Shrivastava S, Paila YD, Kombrabail M, Krishnamoorthy G, Chattopadhyay A (2020) Role of cholesterol and its immediate biosynthetic precursors in membrane dynamics and heterogeneity: implications for health and disease. J Phys Chem B 124(29):6312–6320
- Skrede S, Bjorkhem I, Buchmann MS, Hopen G, Fausa O (1985) A novel pathway for biosynthesis of cholestanol with 7 alphahydroxylated C27-steroids as intermediates, and its importance for the accumulation of cholestanol in cerebrotendinous xanthomatosis. J Clin Invest 75(2):448–455

- Spann NJ, Glass CK (2013) Sterols and oxysterols in immune cell function. Nat Immunol 14(9):893–900
- Stevens MM, Honerkamp-Smith AR, Keller SL (2010) Solubility limits of cholesterol, lanosterol, ergosterol, stigmasterol, and beta-sitosterol in electroformed lipid vesicles. Soft Matter 6(23):5882–5890
- Sviridov D, Mukhamedova N, Miller YI (2020) Lipid rafts as a therapeutic target. J Lipid Res 61(5):687–695
- Wang J, Megha E (2004) London, relationship between sterol/steroid structure and participation in ordered lipid domains (lipid rafts): implications for lipid raft structure and function. Biochemistry 43(4):1010–1018
- Wielkoszynski T, Zalejska-Fiolka J, Strzelczyk JK, Owczarek AJ, Cholewka A, Kokoszczyk K, Stanek A (2020) 5alpha,6alphaepoxyphytosterols and 5alpha,6alpha-epoxycholesterol increase nitrosative stress and inflammatory cytokine production in rats on low-cholesterol diet. Oxid Med Cell Longev 2020:4751803
- Winkler MBL, Kidmose RT, Szomek M, Thaysen K, Rawson S, Muench SP, Wustner D, Pedersen BP (2019) Structural insight into eukaryotic sterol transport through niemann-pick type C proteins. Cell 179(2):485-497 e18
- Xu X, London E (2000) The effect of sterol structure on membrane lipid domains reveals how cholesterol can induce lipid domain formation. Biochemistry 39(5):843–849
- Yamauchi Y, Rogers MA (2018) Sterol metabolism and transport in atherosclerosis and cancer. Front Endocrinol (lausanne) 9:509
- Zmyslowski A, Szterk A (2019) Oxysterols as a biomarker in diseases. Clin Chim Acta 491:103–113

Publisher's Note Springer Nature remains neutral with regard to jurisdictional claims in published maps and institutional affiliations.

Authors and Affiliations

Ursula Perez-Salas¹ · Lionel Porcar² · Sumit Garg¹ · Manuela A. A. Ayee³ · Irena Levitan⁴

- Physics Department, University of Illinois at Chicago, Chicago, IL 60607, USA
- Institut Laue Langevin, 71 Avenue des Martyrs, 38042 Grenoble Cedex 9, France
- Department of Engineering, Dordt University, Sioux Center, IA, USA
- Division of Pulmonary, Critical Care, Sleep and Allergy, Department of Medicine, University of Illinois at Chicago, Chicago, IL 60607, USA

